PHYSOR 2004 - the Physics of Fuel Cycles and Advanced Nuclear Systems: Global Developments
Chicago, Illinois, April 25-29, 2004, on CD-ROM, American Nuclear Society, Lagrange Park, IL. (2004)

A Mutual Resonance Shielding Model Consistent with Ribon Subgroup Equations

A. HÉBERT*
Institut de génie nucléaire, École Polytechnique de Montréal
C.P. 6079, succ. Centre-ville, Montréal, Québec, CANADA H3C 3A7

The paper describes the improvement of the lattice code component related to resonance self-shielding calculations. A new numerical scheme is proposed to represent the mutual shielding effect of overlapping resonances between different isotopes, in the context of the Ribon subgroup equations. The interference effects between two resonant isotopes are represented by a correlated weight matrix computed using a CALENDF approach. The model was designed with the primary goal of reducing the CPU ressources required to obtain the solution.

Finally, a validation is presented for the case of a mixture of ^{238}U and ^{240}Pu isotopes located in different geometries. The isotopic absorption rates obtained with the proposed numerical scheme are compared with exact values obtained using a fine-group elastic slowing-down calculation in the resolved energy domain.

KEYWORDS: Resonance Self-Shielding Model, Subgroup Equations, Mutual Shielding Effect, Lattice Calculation

1. Introduction

A self-shielding model is required in any lattice code in order to take into account the resonant behaviour of the cross sections with an energy discretization based on a limited number of groups (between 50 and 200).

The main problem considered in the resonance self-shielding model is how to use self-shielded cross section and probability table information, as retrieved from the isotopic cross-section library. The final objective is to evaluate $\tilde{\sigma}_{\rho,g}$, the microscopic self-shielded cross section for any reaction ρ in group g, which is formally defined as

$$\tilde{\sigma}_{\rho,g} = \mu_g \frac{\int_{u_{g-1}}^{u_g} du\, \sigma_\rho(u)\, \phi(u)}{\int_{u_{g-1}}^{u_g} du\, \phi(u)} = \mu_g \frac{\langle \sigma_\rho \phi \rangle_g}{\langle \phi \rangle_g} \tag{1}$$

where

$u_{g-1}, u_g =$ lethargy limits of group g

*E-mail: alain.hebert@polymtl.ca, Tel. 514-340-4711 (4519)

$\mu_g =$ SPH factor obtained from the multigroup equivalence procedure

$\phi(u) =$ neutron flux inside the resonances

$\sigma_\rho(u) =$ microscopic cross section for nuclear reaction ρ.

The self-shielding phenomenon can be explained from the observation that the cross sections belonging to energy group g may include many resonances. Consequently, both $\sigma_\rho(u)$ and $\phi(u)$ exhibit resonant behavior with peaks and minima in opposite directions. Moreover, $\phi(u)$ also exhibit minima corresponding to resonances from other isotopes. The mutual resonance shielding phenomena occurs when resonances from two different isotopes are overlapping.

Interference effects exist in pressurized water reactor (PWR) fuel:

- between the 20.9 eV resonance of ^{238}U and the 20.45 eV resonance of ^{240}Pu,
- between the 66.0 eV resonance of ^{238}U and the 66.2 eV resonance of ^{240}Pu.

As pointed out by Bernard and Santamarina, mutual shielding modeling in deterministic codes remains a crucial calculation challenge to meet the required target accuracy for LWR-MOX design parameters, such as conversion factor and fuel temperature coefficient.[1] These errors also affect the buildup of ^{241}Pu with burnup.

A multi-year research program was initiated to improve the self-shielding representation in the lower part of the resolved energy domain. We propose to use a new self-shielding model based on the theory of probability tables, as introduced by P. Ribon *et al.* in Refs. 2, 3 and 4. In this approach, a new type of correlated probability table is been used to take into account the slowing-down effects at low energy. Detailed cross-section information for the total and P_0 scattering reactions, known as *Autolib data* is been used to compute these probability tables in the resolved energy domain. The case corresponding to a single resonant isotope was treated in Ref. 5. The current paper is a generalization dedicated to the multi-isotope case. The new method has been implemented in a development version of the lattice code DRAGON.[6]

2. Description of the Mutual Resonance Shielding Model

The collision probability form of the transport equation can be used to describe an heterogeneous case. In a two resonant isotopes case, we obtain

$$\phi_i(u) = \sum_{j=1}^{I} p_{ij}(u) \left(\Sigma^+_{\mathrm{s},j} + N^{*a}_j \, \mathbf{r}^a_j\{\phi_j(u)\} + N^{*b}_j \, \mathbf{r}^b_j\{\phi_j(u)\} \right) \quad , \quad i = 1, I \tag{2}$$

where I is the number of regions, $p_{ij}(u)$ is a lethargy-dependent reduced collision probability, $\Sigma^+_{\mathrm{s},j}$ is the macroscopic P_0 scattering cross section of the non–resonant isotopes in region j, N^{*a}_j and N^{*b}_j are the number density of the two resonant isotopes in region j. $\mathbf{r}^a_j\{\phi_j(u)\}$ and $\mathbf{r}^b_j\{\phi_j(u)\}$ are the slowing down operators, as defined in Ref. 5. The collision probability matrix can be conveniently merged into a $I = I^* + 1$ order matrix, where I^* is the number of resonant mixtures, without loosing accuracy.

Probability tables are next calculated for both resonant isotopes, as described in Ref. 5. K^a and K^b subgroups are used for each isotope, respectively. Correlated weight matrices $\omega^a_{k,\ell}$ and $\omega^b_{k,\ell}$ are

computed to represent the correlation of the slowing-down source on each isotope considered as unique. We also compute $\sigma^{*a}_{\mathrm{w},j,\ell}$ and $\sigma^{*b}_{\mathrm{w},j,\ell}$ as the microscopic secondary scattering cross sections of each resonant isotope in subgroup ℓ and region j.

We now define $\phi^a_{i,k}$ and $\phi^b_{i,k}$ as the flux in region i and subgroup k for isotopes a and b, respectively. The discretized form of the above equation is written

$$\phi^a_{i,k} = \sum_{j=1}^{I} \bar{p}^a_{ij,k} \left(\Sigma^+_{\mathrm{s},j} + N^{*a}_j \sum_{\ell=1}^{K^a} \frac{\omega^a_{k,\ell}}{\omega^a_k} \, \sigma^{*a}_{\mathrm{w},j,\ell} \, \phi^a_{j,\ell} + N^{*b}_j \sum_{\ell=1}^{K^b} \omega^b_\ell \, \sigma^{*b}_{\mathrm{w},j,\ell} \, \phi^b_{j,\ell} \right) \quad ; \; 1 \le k \le K^a \tag{3}$$

and

$$\phi^b_{i,k} = \sum_{j=1}^{I} \bar{p}^b_{ij,k} \left(\Sigma^+_{\mathrm{s},j} + N^{*a}_j \sum_{\ell=1}^{K^a} \omega^a_\ell \, \sigma^{*a}_{\mathrm{w},j,\ell} \, \phi^a_{j,\ell} + N^{*b}_j \sum_{\ell=1}^{K^b} \frac{\omega^b_{k,\ell}}{\omega^b_k} \, \sigma^{*b}_{\mathrm{w},j,\ell} \, \phi^b_{j,\ell} \right) \quad ; \; 1 \le k \le K^b \tag{4}$$

where $\bar{p}^a_{ij,k}$ and $\bar{p}^a_{ij,k}$ are components of averaged collision probability matrices computed in such a way to take into account the interference effects between isotopes a and b. These calculations can be performed in an efficient way by using correlated weight matrices $\omega^{ab}_{k,\ell}$, relating the total cross sections for isotopes a and b, and obtained using the CALENDF approach of Ref. 7. These weight matrices are computed in such a way that

$$\sum_{\ell=1}^{K^b} \omega^{ab}_{k,\ell} = \omega^a_k \quad \text{and} \quad \sum_{\ell=1}^{K^a} \omega^{ab}_{\ell,k} = \omega^b_k \ .$$

The collision probability components

$$\bar{p}^a_{ij,k} = \sum_{\ell=1}^{K^b} \frac{\omega^{ab}_{k,\ell}}{\omega^a_k} \, p_{ij,k\ell} \quad \text{and} \quad \bar{p}^b_{ij,k} = \sum_{\ell=1}^{K^a} \frac{\omega^{ab}_{\ell,k}}{\omega^b_k} \, p_{ij,\ell k} \tag{5}$$

may be computed using the macroscopic cross sections

$$\Sigma_{i,k\ell} = \Sigma^+_i + N^{*a}_i \sigma^{*a}_{i,k} + N^{*b}_i \sigma^{*b}_{i,\ell} \ , \quad i = 1, I \ . \tag{6}$$

Obtaining $\bar{p}^a_{ij,k}$ and $\bar{p}^b_{ij,k}$ from Eqs. (5) and (6) requires $K^a \times K^b$ individual collision probability calculations, a large number which can be even larger if more than two resonant isotopes are correlated. The proposed solution consists in using a dilution-matrix approximation for representing the components $p_{ij,k\ell} = p_{ij}(\sigma^{*a}_k, \sigma^{*b}_\ell)$.

We first address the calculation of matrix components $\bar{p}^a_{ij,k}$ from Eq. (5), taking into account the correlation effect. Introducing the dilution matrix approximation:

$$\boldsymbol{p}^{*a}_{k\ell} = [\boldsymbol{E}^{*a}_k + \boldsymbol{\Sigma}^*_{k\ell}]^{-1} \ , \ \ k = 1, K^a \text{ and } \ell = 1, K^b \tag{7}$$

where $\boldsymbol{p}^{*a}_{k\ell} = \{p_{ij,k\ell}\,, \ i = 1, I \text{ and } j = 1, I\}$ and $\boldsymbol{\Sigma}^*_{k\ell} = \mathrm{diag}\{N^{*a}_i \sigma^{*a}_{i,k} + N^{*b}_i \sigma^{*b}_{i,\ell}\,, \ i = 1, I\}$. The set of K^a multiband dilution matrices $\boldsymbol{E}^{*a}_k$ can be computed in such a way to preserve the value of $\bar{p}^a_{ij,k}$ obtained without any correlation model. In this case, we would have $\bar{p}^a_{ij,k} = p_{ij}(\sigma^{*a}_k, \bar{\sigma}^{*b})$ where

the averaged total cross section of isotope b is obtained from the multiband flux $\phi^b_{i,\ell}$ of the previous iteration:

$$\bar{\sigma}^{*b}_i = \frac{\sum\limits_{\ell} \omega^b_\ell \, \sigma^{*b}_{i,\ell} \, \phi^b_{i,\ell}}{\sum\limits_{\ell} \omega^b_\ell \, \phi^b_{i,\ell}} \quad . \tag{8}$$

The set of K^a multiband dilution matrices $\boldsymbol{E}^{*a}_k$ is computed in matrix algebra by solving the following non-linear equation:

$$\bar{\boldsymbol{p}}^{*a}_k = \sum_{\ell=1}^{K^b} \omega^b_\ell \, \boldsymbol{p}^{*a}_{k\ell} = \sum_{\ell=1}^{K^b} \omega^b_\ell \, [\boldsymbol{E}^{*a}_k + \boldsymbol{\Sigma}^*_{k\ell}]^{-1} \tag{9}$$

where $\bar{\boldsymbol{p}}^{*a}_k = \{p_{ij}(\sigma^{*a}_k, \bar{\sigma}^{*b}) \, , \; i = 1, I \text{ and } j = 1, I\}$ and $\bar{\boldsymbol{\Sigma}}^{*a}_k = \text{diag}\{N^{*a}_i \sigma^{*a}_{i,k} + N^{*b}_i \bar{\sigma}^{*b}_i \, , \; i = 1, I\}$.

The solution of Eq. (9) is obtained using the following fixed point iteration:

$$\begin{aligned} (\boldsymbol{E}^{*a}_k)^{(0)} &= [\bar{\boldsymbol{p}}^{*a}_k]^{-1} - \bar{\boldsymbol{\Sigma}}^{*a}_k \\ (\boldsymbol{E}^{*a}_k)^{(n+1)} &= (\boldsymbol{E}^{*a}_k)^{(n)} + [\bar{\boldsymbol{p}}^{*a}_k]^{-1} - \left[\sum_{\ell=1}^{K^b} \omega^b_\ell \left[(\boldsymbol{E}^{*a}_k)^{(n)} + \boldsymbol{\Sigma}^*_{k\ell} \right]^{-1} \right]^{-1} \quad , \;\; n \geq 0 \end{aligned} \tag{10}$$

where $k = 1, K^a$.

The above iterative procedure usually converges in less than five iterations. Using the components of Eq. (7), the term inside the summation operator in Eq. (5) only involve a $(I^* + 1)-$order matrix inversion; it does not involve any collision probability calculation and can therefore be computed efficiently.

A few outer iterations are also required to converge on asymptotic values of $\phi^a_{i,k}$ and $\phi^b_{i,k}$ using Eqs. (3) and (4). The number of collision probability matrix calculations related to an energy group is equal to $(K^a + K^b) \times N$ where N is the number of outer iterations. If one-speed flux solution operators are used instead of integrating collision probabilities, a collision probability matrix can be computed using $I^* + 1$ flux calculations, where I^* is the number of resonant mixtures. In this case, the number of flux calculations related to an energy group is equal to $(I^* + 1) \times (K^a + K^b) \times N$. After convergence of multiband fluxes $\phi^a_{i,k}$ and $\phi^b_{i,k}$, self-shielded cross sections may be computed as before.[5]

3. Numerical Results

Two computer codes have been used to implement this new self-shielding model:

1. A computer code, named CESCOL, makes it possible to solve a fixed-source slowing-down equation using an elastic slowing-down operator for a mixture of heavy (resonant) isotopes in the resolved energy domain.[8] A homogeneous option is available and can be used to produce cross section tabulated data that can be interpolated in dilution. Heterogeneous cases can also be treated using CP techniques and used to generate reference solutions. CESCOL is used to produce both the reference solution and the cross section tabulated data at selected dilutions. We choose a set of dilutions σ_e between 1.5 barn and 10000.0 barn containing $L = 18$ finite values equally spaced on a logarithmic scale. Infinite dilution (1.0×10^{10} barns) was also selected.

2. A self-shielding module was written in a development version of the DRAGON lattice code[6], based on the subgroup model of Ref. 5 with the mutual resonance shielding model presented in this paper. Self-shielded cross sections are obtained for a coarse energy grid and used in the existing CP flux solution module. Consistency is emphasized by using the same CP calculation module in both heterogeneous CESCOL and lattice code calculations.

The validation tests presented in this study are limited to the resolved energy domain where it is possible to precisely define the resonant cross sections. Cross sections were defined in the resolved energy domain and distributed over APOLLO-1 energy groups 31 to 52, located between 2.7679 and 677.3 eV. The definition of this mesh is shown in Fig. 1. A 1.0 n/cm^3·s source was placed in group number 31, located between 454 eV and 677.3 eV. We studied the absorption rates for the resonant isotopes in energy groups 33 to 52 and reported the discrepancies between CESCOL and lattice code calculations for a set of four benchmarks, similar to those of Ref. 8, containing a mixture of ^{238}U and ^{240}Pu.

Table 1: Isotopic data for Benchmarks 1, 2, 3 and 4^a.

Mixture	Isotope	Density (10^{24} atom/cc)	Temperature (K)
1	^{238}U	2.2×10^{-2}	973.16
	^{240}Pu	8.7×10^{-4}	
	^{16}O	4.574×10^{-2}	
2	Natural Cr	1.48×10^{-2}	
	^{55}Mn	9.0×10^{-4}	
	Natural Fe	5.3×10^{-2}	
	Natural Ni	6.9×10^{-3}	
3	^{1}H	5.0×10^{-2}	
	^{16}O	2.5×10^{-2}	

(a) Benchmarks 1 and 2 use only mixtures 1 and 3

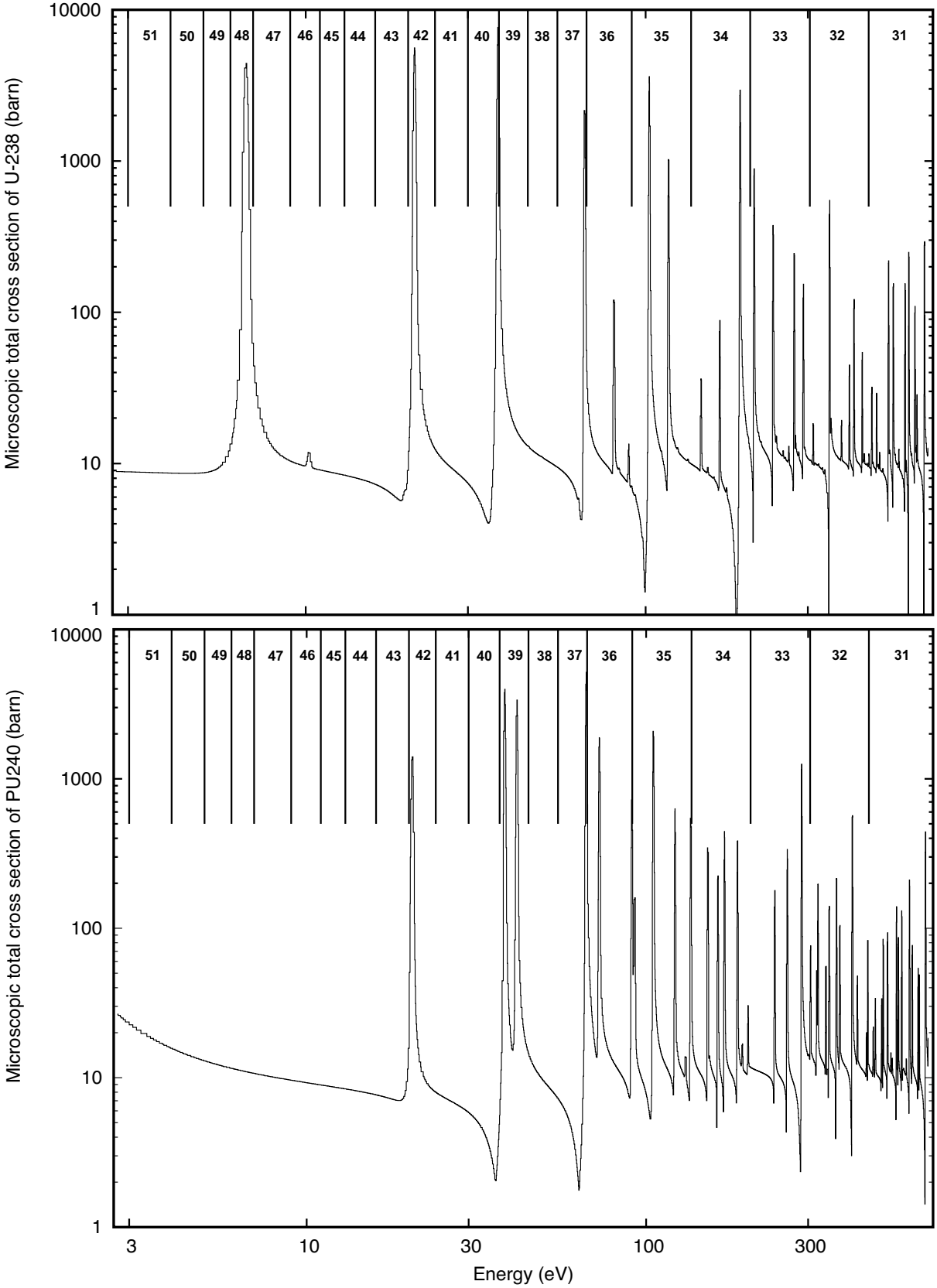

Figure 1: Microscopic fine group total cross sections for ^{238}U and ^{240}Pu.

1. A pure homogeneous case made of a mixture of ^{238}U (2.2×10^{22} atom/cc),^{240}Pu (8.7×10^{20} atom/cc), oxygen (7.074×10^{22} atom/cc) and hydrogen (5.0×10^{22} atom/cc).

2. This Benchmark is a pure two-region cylindrical geometry with radii of 0.4095 and 0.7054 cm. The inner cylinder contains the fuel, a mixture of ^{238}U (2.2×10^{22} atom/cc),^{240}Pu (8.7×10^{20} atom/cc) and oxygen (4.574×10^{22} atom/cc) whereas the outer cylinder contains light water (2.5×10^{22} molecule/cc).

3. This heterogeneous Benchmark represents a simplified 5×5 PWR assembly featuring a water hole surrounded by square and rectangular fuel cells that include cladded fuel rods of different diameters. The fuel, clad and coolant properties are defined in Table 1. CPs for this Benchmark were obtained using the EURYDICE-2[9] module available in both CESCOL and in the lattice code.

4. The fourth Benchmark was set to study the distributed self shielding effects within the fuel rod. The fuel rod is subdivided into six annular volumes and the absorption rate is computed in each subvolume. The annular radii are: 0.25899, 0.34261, 0.36627, 0.38849, 0.39913 and 0.4095 cm. The non-resonant cladding (mixture 2) and moderator have radii equal to 0.4750 and 0.710879 cm, respectively.

The absorption rates obtained using our self-shielding model are compared in Table 2 to reference CESCOL results and a maximum $\epsilon^{\max}$, averaged $\bar{\epsilon}$ and integrated error ϵ^{int} are computed for each numerical test. The main purpose of the numerical tests was to compare the proposed mutual resonance shielding model (*new correlation model*) with calculations performed without taking this phenomena into account (*no correlation*).

Table 2: Summary of Benchmark results.

		no correlation				new correlation model			
	Benchmark	1	2	3	4	1	2	3	4
^{238}U + ^{240}Pu	ϵ^{int} (%)	1.8	2.2	2.7	3.3	-0.7	0.2	0.5	0.5
	$\bar{\epsilon}$ (%)	2.6	3.2	3.3	3.8	1.5	1.4	1.5	1.6
	$\epsilon^{\max}$ (%)	17.5	19.5	19.8	21.8	9.4	6.0	6.2	8.3
	in group	37	37	37	37	37	37	43	43
^{238}U	ϵ^{int} (%)	0.3	0.7	1.1	1.9	-0.9	-0.1	0.2	0.2
	$\bar{\epsilon}$ (%)	1.6	2.0	2.1	2.7	2.0	1.8	1.9	2.0
	$\epsilon^{\max}$ (%)	9.6	11.7	13.5	14.9	10.1	7.2	9.0	10.7
	in group	43	43	43	43	37	35	43	43
^{240}Pu	ϵ^{int} (%)	10.4	11.1	11.9	11.7	0.6	1.8	1.9	2.3
	$\bar{\epsilon}$ (%)	18.1	20.6	21.1	22.3	2.4	2.8	2.8	3.4
	$\epsilon^{\max}$ (%)	145.4	167.6	171.3	186.0	12.0	15.5	16.6	20.0
	in group	42	42	42	42	40	40	40	40

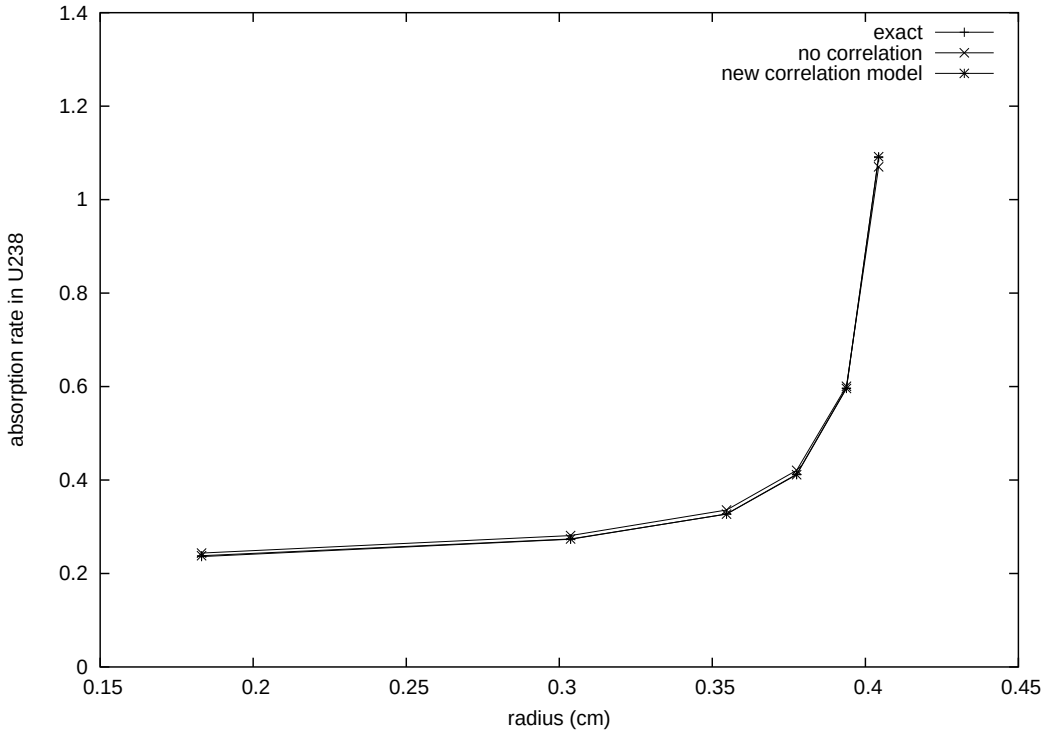

Figure 2: ^{238}U rim effect in fuel rod for Benchmark 4.

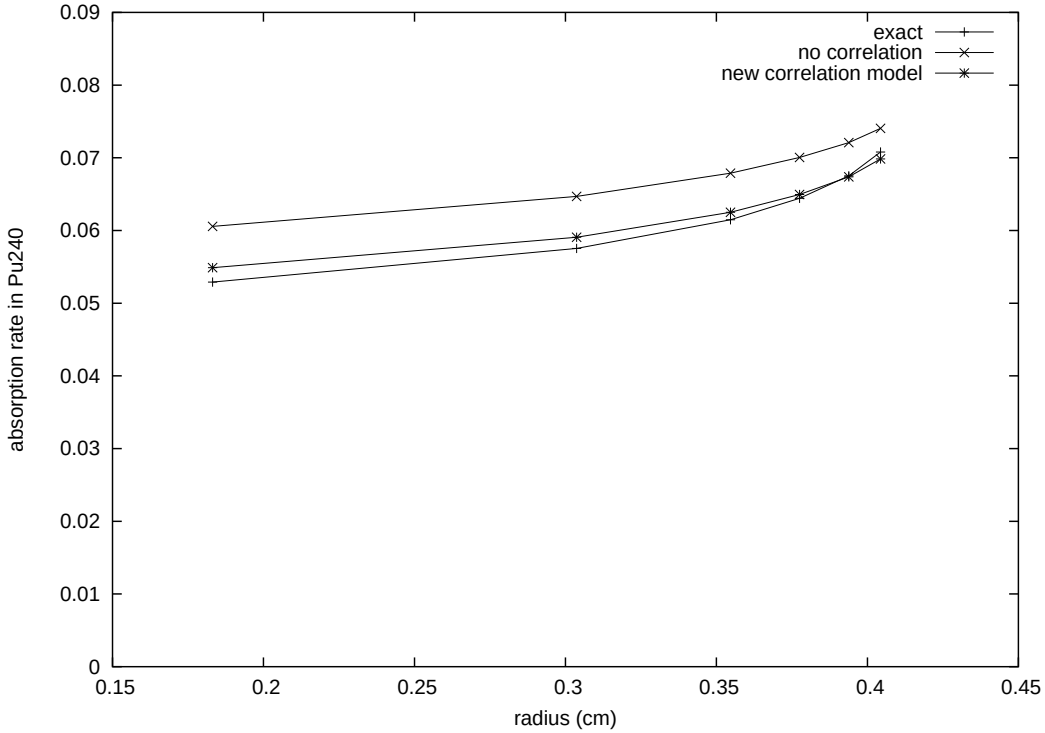

Figure 3: ^{240}Pu rim effect in fuel rod for Benchmark 4.

The spatial distribution of the absorption rates in ^{238}U and ^{240}Pu for Benchmark 4 are plotted in Figs. 2 and 3, respectively. We observe a small improvement on integrated ^{238}U rate errors (from 3.2% to 0.7%) and a more important improvement on ^{240}U rates errors (from 14.5% to 3.7%). The improved curve for ^{238}U is almost indistinguishables from the reference.

4. Conclusions

We have succussfully developed a mutual resonance shielding model based on the rigorous probability table theory of Dr. P. Ribon. This method is highly more accurate than the current approaches which neglect the correlation effects between different resonant isotopes. Moreover, the increase in CPU ressources required by the new model is small. The distributed self-shielding effects are accurately taken into account.

However, more work is required before switching to this new method. We first have to investigate its compatibility with existing cross-section libraries and show its accuracy on the Rowland's Benchmarks.[7, 10] Finally, we have to test its behaviour on depletion cases, as the overall reactivity loss is closely related to the self-shielding accuracy.

Acknowledgements

The author is grateful to Dr. Alain Santamarina of the Commissariat à l'Énergie Atomique (France) for a discussion that motivate this study.

This work was supported by a grant from the Natural Science and Engineering Research Council of Canada.

References

[1] D. Bernard and A. Santamarina, "Doppler Calculation Challenge in MOX Lattices Qualification on Minerve Oscillation Experiment", *Proc. Int. Mtg. on Nuclear Mathematical and Computational Sciences*, Gatlinburg, Tennessee, April 6–11, 2003.

[2] P. Ribon et J.-M. Maillard, "Les tables de probabilité. Application au traitement des sections efficaces pour la neutronique", Note CEA–N–2485, Commissariat à l'Énergie Atomique, Juin 1986.

[3] P. Ribon, "Statistical Probability Tables. CALENDF Program," *Proc. of the Seminar on NJOY and THEMIS*, Saclay, France, June 20-21, 1989, p.220 – 232, OECD/NEA Data Bank (1989).

[4] B. Oum Keltoum Aziza and P. Ribon, "Tables de probabilité non statistiques. Description des effets du ralentissement", *Proc. Int. Conf. on the Physics of Reactors: Operation, Design and Computation*, Marseille, France, April 23 – 27, 1990.

[5] A. Hébert, "Development of a New Resonance Self-Shielding Methodology Based on Probability Table Information", *Proc. Int. Mtg. on Nuclear Mathematical and Computational Sciences*, Gatlinburg, Tennessee, April 6 – 11, 2003.

[6] G. Marleau, A. Hébert and R. Roy, "New Computational Methods Used in the Lattice Code Dragon," *Proc. Int. Top. Mtg. on Advances in Reactor Physics*, Charleston, USA, March 8-11, 1992.

[7] A. Hébert and M. Coste, "Computing Moment-Based Probability Tables for Self-Shielding Calculations in Lattice Codes", *Nucl. Sci. Eng.*, **142**, 245 (2002).

[8] A. Hébert and G. Marleau, "Generalization of the Stamm'ler Method for the Self-Shielding of Resonant Isotopes in Arbitrary Geometries," *Nucl. Sci. Eng.*, **108**, 230 (1991).

[9] A. Hébert, "Développement de la methode SPH: Homogénéisation de cellules dans un réseau non uniforme et calcul des paramètres de réflecteur," CEA- N-2209, Commissariat à L'Énergie Atomique, France (1981).

[10] J. Rowlands et al, "LWR Pin Cell Benchmark Intercomparisons. An Intercomparison study organized by the JEF Project, with contributions by Britain, France, Germany, The Netherlands, Slovenia and the USA.," *JEF Report to be published* , OECD/NEA Data Bank (1999).